Coastal Dynamics 2017
Paper No. 174

RANS-BASED NUMERICAL SIMULATION OF WAVE-INDUCED SHEET-FLOW TRANSPORT OF GRADED SEDIMENTS

David R. Fuhrman[1] and Ugur Caliskan[2]

Abstract

An existing one-dimensional vertical (1DV) turbulence-closure flow model, coupled with sediment transport capabilities, is extended to incorporate graded sediment mixtures. The hydrodynamic model solves the horizontal component of the incompressible Reynolds-averaged Navier–Stokes (RANS) equations coupled with k–ω turbulence closure. In addition to standard bed and suspended load descriptions, the sediment transport model incorporates so-called high-concentration effects (turbulence damping and hindered settling velocities). The sediment transport model treats the bed and suspended load individually for each grain fraction within a mixture, and includes effects associated with increased exposure of larger particles within a mixture. The model also makes use of a modified reference concentration approach, with reference concentrations computed individually for each fraction, and then translated to a common level, which conveniently enables use of a single computational grid for the simulation of suspended sediments. Parametric study shows that these effects combine to help alleviate an otherwise systematic tendency towards over- and under- predicted transport rates for fine and coarse sand fractions, respectively. The sediment transport model is validated against experimental sheet-flow measurements conducted in oscillatory tunnels beneath velocity-skewed wave signals, and demonstrates similar accuracy (predicted transport rates generally within a factor of two of measurements) for both graded mixtures and uniform sands.

Key words: sediment transport, graded sediments, non-uniform sediment mixtures, wave boundary layer, k-ω turbulence model

1. Introduction

In nearshore coastal environments under storm conditions bed ripples are typically washed out, and sediments are transported within a thin O(1 cm) layer above the bed. Cross-shore sediment transport processes under such so-called sheet flow conditions have been the focus of much recent experimental and numerical research. Extensive experimental work in oscillating tunnels has led e.g. to the databases presented by e.g. van der Werf et al. (2009) and Silva et al. (2011). Models for predicting sheet-flow sediment transport rates induced by waves vary considerably in complexity, ranging from: (1) relatively simple quasi-steady approaches (e.g. Nielsen and Callaghan, 2003), (2) intermediately-complex turbulence closure-based methods (e.g. Davies and Li 1997, Holmedal and Myrhaug 2006), to (3) very detailed two-phase approaches (e.g. Amoudry et al. 2008).

The vast majority of research involving sediment transport beneath waves has focused on experiments or numerical models based on uniform grained (well-sorted) sediments, with relatively limited emphasis on related processes involving graded sediments. Experimental work involving transport of graded sands beneath velocity-skewed wave signals in oscillatory tunnel environments include those of e.g. O'Donoghue and Wright (2004) and Hassan and Ribberink (2005). Methods for modeling wave-induced transport of sediment mixtures include the works of van Rijn (2007), who highlighted the importance of incorporating hiding/exposure corrections factors for calculating transport rates on graded beds, as well as the practical approaches developed recently by e.g. van der A et al. (2013) and Wu and Lin (2014). Published attempts at 1DV (one-dimensional vertical) turbulence closure based modeling of graded sediments beneath waves are quite limited, seemingly to that of Li and Davies (2001), on which the present work builds.

This paper is an abridged version of a full journal article, recently published in Caliskan and

[1]Technical University of Denmark, Department of Mechanical Engineering, Denmark. drf@mek.dtu.dk
[2]Technical University of Denmark, Department of Mechanical Engineering, Denmark.

Fuhrman (2017). Selected excerpts and figures reproduced herein are with permission from Elsevier.

2. Model Description

2.1. *Hydrodynamic model*

The basic hydrodynamic model utilized in the present work is based on the horizontal component of the Reynolds-averaged Navier-Stokes equations, coupled with two-equation k-ω turbulence closure (Wilcox 2006). The model is of the one-dimensional-vertical (1DV) type, meaning that it requires (finite difference) discretization of only a single vertical line. The model flow is driven by a user-prescribed pressure gradient, which can be utilized to simulate e.g. velocity signals that are commonly utilized within oscillatory tunnel environments. For the sake of brevity, the flow model will not be described in more detail here, and for full details the interested reader is referred to Fuhrman et al. (2013) and Caliskan and Fuhrman (2017).

2.2. *Sediment transport model*

The sediment transport model extends the uniform grain size sediment transport capabilities originally described in Fuhrman et al. (2013) to handle multiple grain fractions, with each fraction handled individually in a manner similar to Li and Davies (2001), though different in detail. The sediment transport model includes both bed and suspended load descriptions, described separately below.

2.2.1. *Bed load model*

In the present approach, the rate of bed load transport for the i-th grain fraction comprising a mixture, $q_{B,i}$, is calculated based on the formula of Engelund and Fredsøe (1976):

$$\Phi_{B,i} = \frac{q_{B,i}}{\sqrt{(s-1)gd_i^3}} = 5p_i\left(\sqrt{\theta_i} - 0.7\sqrt{\theta_c}\right) \tag{1}$$

where the (weighted) probability of moving grains is given by:

$$p_i = w_{f,i}\left[1+\left(\frac{\pi\mu_d}{6(\theta_i-\theta_c)}\right)^4\right]^{-\frac{1}{4}} \tag{2}$$

Here θ_c=0.045 is the critical Shields parameter corresponding to incipient motion conditions, taken as constant for simplicity. In the above, $w_{f,i}$ corresponds to the i-th weight fraction comprising a graded sediment mixture. Note that, in contrast to the model of Li and Davies (2001), equal fractions are not necessarily assumed. The coefficient of dynamic friction is taken to be μ_d = 0.65. For each grain fraction, the effective Shields parameter is defined by

$$\theta_i = \left(\frac{d_i}{d_{50}}\right)^{h_c}\left(\frac{U_f^2}{(s-1)gd}\right) \tag{3}$$

where g=9.81 m/s^2 is gravitational acceleration. In the above h_c represents an exposure factor accounting for larger particles being more exposed to the flow than smaller particles on graded sediment beds. Following van Rijn (2007), a default value h_c = 0.25 is used, unless otherwise noted. Note that the effect of this parameter can easily be switched off simply by setting h_c = 0.

2.2.2. *Suspended load model*

The hydrodynamic model is likewise coupled with a turbulent-diffusion description for the simulation of the suspended sediment concentrations. The concentration representing each weight fraction is simulated individually according to:

$$\frac{\partial c_i}{\partial t} = \frac{\partial \left(w_{s,i} c_i \right)}{\partial y} + \frac{\partial}{\partial y}\left(\varepsilon_s \frac{\partial c_i}{\partial y} \right), \quad \varepsilon_s = \beta_s \nu_T + \nu \tag{4}$$

where $w_{s,i}$ is the settling velocity of the i-th grain fraction, calculated according to the method presented in Fredsøe and Deigaard (1992), ε_s is the diffusion coefficient, and ν_T is the eddy viscosity obtained from the turbulence closure model. The molecular viscosity is included purely for numerical reasons. In what follows the value β_s=2 is utilized. Eq. (4) is solved for $b \le y \le h_m$, where b=2d_{50} is taken the as the fixed reference level and h_m is the total model height. The calculation of the instantaneous rate of suspended sediment transport for each fraction is made according to:

$$q_{S,i} = \int_b^{h_m} u c_i dy, \quad b = 2d_{50} \tag{5}$$

Reference concentrations are imposed at the lower y=b boundary, as follows. Specifically, the reference concentration formula of Zyserman and Fredsøe (1994a) will be utilized:

$$c_{b0,i} = w_{f,i} \frac{0.331 \left(\theta_i - \theta_c \right)^{1.75}}{1 + \frac{0.331}{0.32} \left(\theta_i - \theta_c \right)^{1.75}} \tag{6}$$

where the maximum concentration is modified from 0.46 to 0.32, as suggested by Zyserman and Fredsøe (1994b) for oscillatory flows. Note that rather than being based on the median grain size d_{50}, as suggested in these original works, in the present work the reference concentration will be assumed to be valid (on a weighted basis, hence multiplication by $w_{f,i}$ above) for each individual weight fraction. This follows a similar approach as in Li and Davies (2001), who utilized a reference concentration based on the method of Engelund and Fredsoe (1976).

When applied individually for each grain fraction i, it is likewise assumed here that the concentrations computed from (6) will best represent those at the "natural" reference level for each respective grain size, i.e. at y=b_i=2d_i, rather than at the fixed (common) reference level, again here taken as y=b=2d_{50}. To translate the concentrations from (6) from y=b_i to the common reference level y=b (thereby conveniently enabling use of a single computational grid for suspended sediments of all fractions), we then introduce the following additional modification:

$$c_{b,i} = c_{b0,i} \left(\frac{b_i}{b} \right)^{\Gamma}, \quad y = b \tag{7}$$

This modification accounts for the individual "natural" reference levels b_i being higher (lower) than b for larger (smaller) grains. Hence, it will respectively increase (decrease) the amount of sediment put into suspension, relative to direct application of (6) at y=b. Both of these scenarios (i.e. $d_i < d_{50}$ and $d_i > d_{50}$) are demonstrated conceptually in Figure 1. A theoretical basis and further discussion of this modification is presented in Caliskan and Fuhrman (2017), where it is demonstrated that the parameter Γ is closely linked to the Rouse parameter for steady flows. Nevertheless, a default fixed value Γ=1.25 will be used in the present work, for simplicity. Note that this feature can easily be switched off simply by setting Γ=0, then yielding $c_{b,i}$=$c_{b0,i}$, the effect of which will also be demonstrated.

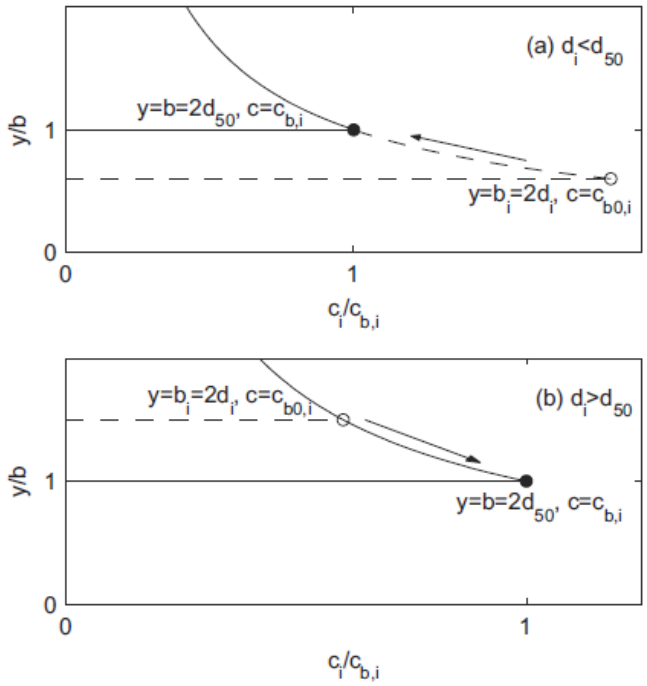

Figure 1. Demonstration of the reference concentration modification utilized in the present approach, resulting in (a) a decreased reference concentration $c_{b,i}$ when $d_i < d_{50}$ and (b) an increased reference concentration $c_{b,i}$ when $d_i > d_{50}$. The open circles represent the concentration at $y=b_i=2d_i$ calculated via (6), whereas the filled circles represent the concentration utilized at the reference level $y=b=2d_{50}$, after application of (7). This figure is reprinted from Caliskan and Fuhrman (2017), with permission from Elsevier.

3. Sediment Transport beneath Skewed Free Stream Velocity Signals

3.1. *Model validation*

In this section we will validate the model presented above against two experimental data sets (O'Donoghue and Wright 2004, Hassan and Ribberink 2005) involving graded sediment transport beneath velocity-skewed wave signals on flat beds within oscillating tunnel facilities. O'Donoghue and Wright (2004, hereafter denoted OW) performed a series of 12 tests, 6 of which utilized well-sorted sediments (fine sand with d=0.15 mm, medium sand with d=0.28 mm, and coarse sand with d=0.51 mm), and 6 of which utilized three sediment mixtures (Mix X1, Mix X2, and Mix X3, having d_{50}=0.19 mm, 0.28 mm, and 0.28 mm, respectively) as indicated in Table 1. Two different wave periods T=5 s and T=7.5 s were likewise considered, in combination with free stream velocities having the form of a 2nd-order Stokes wave, with first and second harmonic amplitudes U_{1m}=1.21 m/s and U_{2m}=0.31 m/s, respectively. For the present purposes, we will consider all 12 of their experimental conditions, hence demonstrating model performance for both graded and well-sorted (uniform) sediments. Comparisons will be limited to the reported period-averaged total transport rates in what follows.

Hassan and Ribberink (2005, hereafter denoted HR) have likewise conducted a series of oscillating tunnel experiments involving sheet flow beneath skewed free-stream velocity signals having similar form. Comparison will therefore also be made against their 19 pure wave cases involving uniform sands (grain diameters ranging from d=0.13 mm to 0.97 mm), corresponding to their B, C, D, R, and Q series (full period results only). These conditions consider wave periods ranging from T=5 s to 12 s. In addition, we will consider their K, P, and S series of tests (a total of 10 cases) utilizing the sediment mixtures indicated in Table 2. For each of their conditions the model is set up such that the free stream flow takes a form consistent with a 2nd-order Stokes wave, with the velocity magnitudes U_{1m} and U_{2m} set in accordance with their reported parameters.

In addition to the total period-averaged transport rate for the sediment mixtures, HR also report the period-averaged transport for each individual weight fraction. Hence, comparison with our model

results will also be attempted for these quantities in what follows, i.e. transport rates both in terms of the total transport, as well as that for each individual weight fraction, will be considered.

Table 1. Sediment mixture descriptions for the experiments of O'Donoghue and Wright (2004).

Mix	d_{50} (mm)	d_i (mm)	$w_{f,i}$
X1	0.19	[0.15, 0.28, 0.51]	[0.60, 0.30, 0.10]
X2	0.28	[0.15, 0.28, 0.51]	[0.20, 0.60, 0.20]
X4	0.28	[0.15, 0.51]	[0.50, 0.50]

Table 2. Considered sediment mixture descriptions for the experiments of Hassan and Ribberink (2005).

Mix	d_{50} (mm)	d_i (mm)	$w_{f,i}$
K	0.194	[0.13, 34]	[0.50, 0.50]
P	0.24	[0.21, 97]	[0.70, 0.30]
S	0.15	[0.13, 0.34, 0.97]	[0.60, 0.20, 0.20]

For all tests considered, the model depth is set to h_m=0.25 m, corresponding to half of the distance from the sand bottom to the roof of the experimental tunnel. The experiments on the sand beds were generally carried out over 25 flow cycles. Thus, for comparison all computed results presented will be taken from the 12th cycle, corresponding approximately to the middle of the experimental duration. Note that beyond the first few cycles the predicted net transport rates vary little (of the order 10%) over the full course of the experimental duration, so the precise cycle considered is not of much significance.

Model validation results for the experimental conditions described above are depicted in Figure 2. In this comparison, all model features are switched on, making use of the previously-indicated default parameters: μ_d=0.65, β_s=2.0, Γ=1.25 and h_c=0.25. In this figure, and in some others that follow, we will maintain the following organization: Subplot (a) presents comparison of computed and measured period-averaged total transport rates (combined bed and suspended load) for individual weight fractions, as reported by HR; subplot (b) presents comparison of the total period-averaged transport of the full mixtures, as reported by HR and OW; finally, subplot (c) presents comparison of the total transport rate for the experiments involving uniform sediments, as reported by both HR and OW. On each subplot, the full line represents the line of perfect agreement, whereas the region between the dashed lines represents agreement within plus or minus a factor of two; while obviously not perfect, this is often taken as acceptable accuracy when making sediment transport predictions.

We will first discuss the comparison of transport rates for the individual grain fractions of HR, which are again presented in Figure 2a. Despite the considerable difficulty in simultaneously predicting the transport of a wide range of sediment sizes (ranging from fine to course sands), the present results appear to be reasonable, with most of the predicted net transport rates being within a factor of two of those measured. In some cases, due to phase lag effects, it is seen that the finest sediments were in fact transported backwards; while the magnitude of negative transport rates for these fine sand fractions tends to be over-predicted by the model, this phenomenon is at least qualitatively captured. On balance, there appears to be a slight tendency towards the over-prediction of transport rates for the finer fractions, and under-prediction for coarser fractions, though exceptions are apparent for each, and both are again approximately within a factor two of measurements.

The general quality of predicting the total sediment transport rates for the full mixtures can be further seen in Figure 2b, now considering both the OW and HR experiments. The HR cases, containing the widest range of grain sizes of the two, are seen to consistently lie close to the line of perfect agreement. The clustering for the prediction of the OW mixture experiments is less impressive, but is still acceptable, with all but two cases being within a factor two (dashed lines). There does also not appear to be any consistent or systematic trend towards either over- or under-predicting the total transport rate for sediment mixtures based on these data sets. All predicted net transports for the mixtures are positive, in line with the experiments.

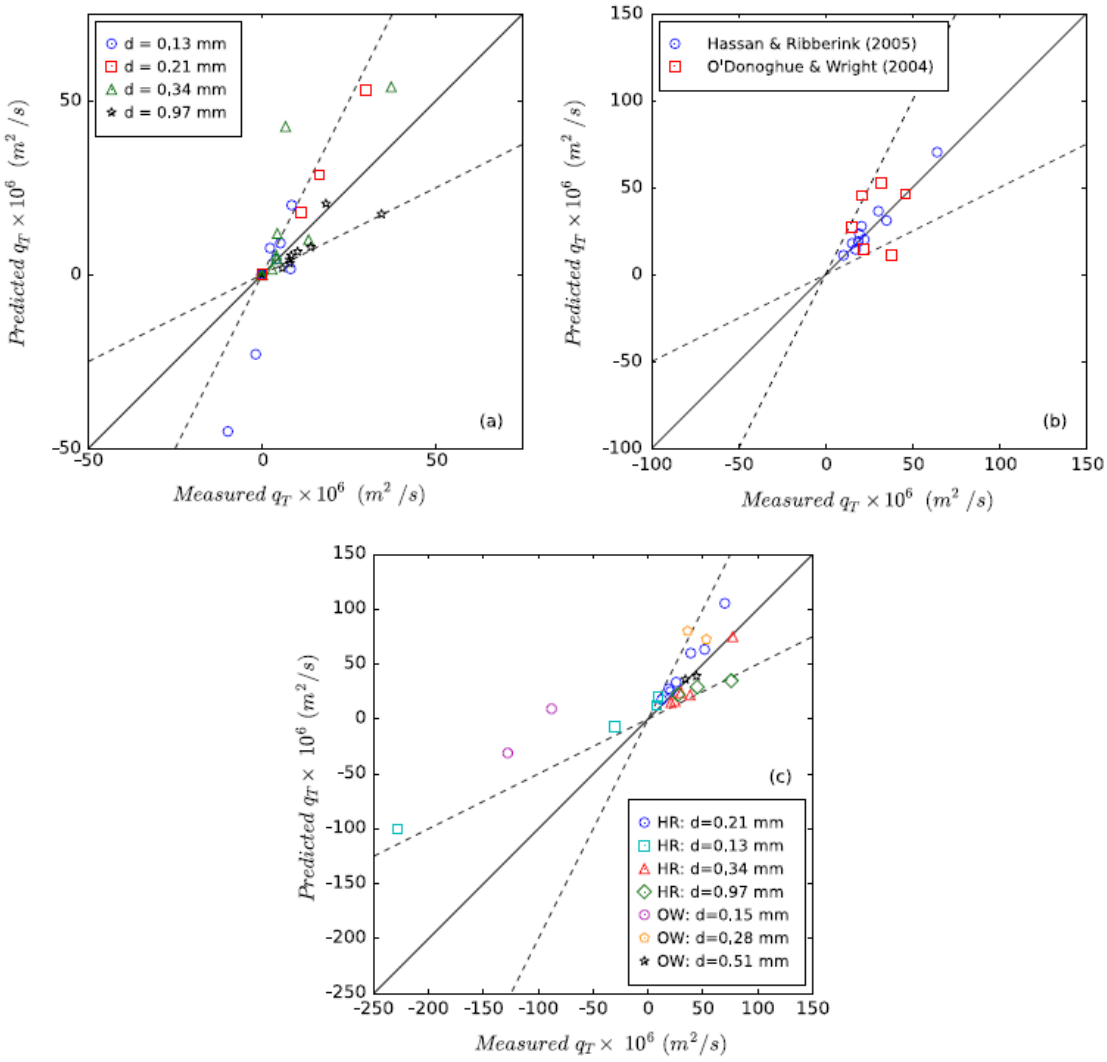

Figure 2. Summary of measured versus predicted period-averaged sediment transport rates, based on skewed wave experiments of HR: Hassan and Ribberink (2005) and OW: O'Donoghue and Wright (2004). Sub-plot (a) compares transport rates for individual weight fractions (from HR), (b) compares total transport rates of mixtures (both HR and OW), and (c) compares total transport rates for uniform sands (both HR and OW). This figure is reprinted from Caliskan and Fuhrman (2017) with permission from Elsevier.

The generally good agreement with the HR data set is further demonstrated in Figure 3, which depicts the total net transport rate versus the third moment of the free stream velocity $\langle u_0 \rangle^3$ for all of their non-uniform sand cases. The present model captures e.g. the linear growth in the net transport for mix P (containing d=0.21 mm and 0.97 mm). The model likewise captures e.g. the deviation from the linear trend for larger $\langle u_0 \rangle^3$, with mix S (mixture containing d=0.13 mm, 0.34 mm, and 0.97 mm). Inspection of the model results indicates that the break in this linear trend for mix S is due to unsteady effects of the fine sand fraction (d=0.13 mm), which is actually transported in the negative direction, again due to the previously-mentioned phase lag effects (this fraction fails to settle completely prior to flow reversal). Indeed, these effects were speculated directly by HR.

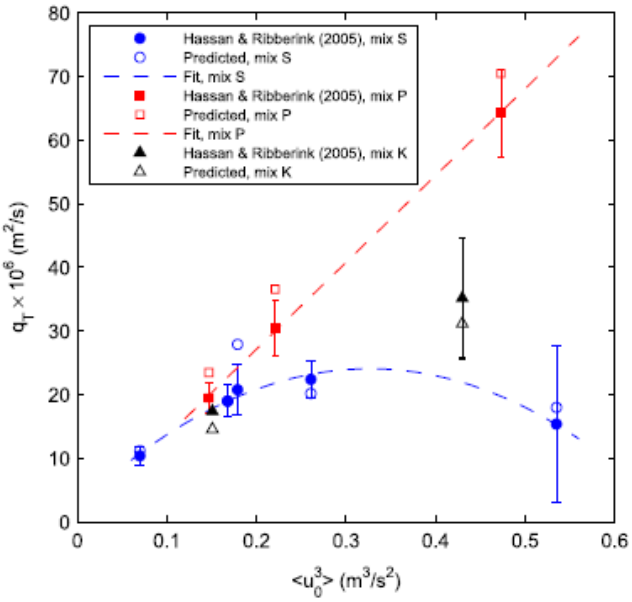

Figure 3. Measured and predicted net sediment transport rates versus the third moment of the free stream velocitys for the non-uniform sand cases from HR. The experimental error bars for each case are also shown. The dashed lines are curve fits to the experimental data from mix S and P. This figure is reprinted from Caliskan and Fuhrman (2017) with permission from Elsevier.

As final validation, we compare computed sediment transport rates with those measured for the well-sorted (uniform grain) sediment beds in Figure 2c. This is an important test, as situations involving uniform sized sediments are obviously special cases of those involving sediment mixtures. As seen, the model is also able to make reasonable predictions in these cases. For the cases involving positive transport, all but two of the predicted transport rates are within a factor of two of the measurements (namely one from OW, with d=0.28 mm and one from HR, with d=0.97 mm). For the fine sand cases demonstrating net negative transport rates (again due to phase lag effects), the model under-estimates the magnitude of the transport, but does captures this phenomenon qualitatively in three of the four cases.

Regarding the importance of phase-lag effects beneath velocity-skewed flows, it is noted that recent numerical results of Fuhrman et al. (2013) and Kranenburg et al. (2013) have revealed that inclusion of progressive wave streaming (and other related convective term effects) can, in fact, "re-reverse" the transport of fine grained sediments in such cases to be in the positive direction. Hence, based on their results, it seems that the phenomenon of negative transport of fine sands beneath skewed wave signals may actually be an experimental artifact caused by the streamwise-uniform nature of flow within oscillating tunnel facilities.

We summarize as follows: the results depicted in Figures 2 and 3 collectively demonstrate the ability of the present model to predict period-averaged wave-induced sediment transport rates for sediment mixtures, involving a wide range of particle sizes (ranging from fine to coarse sands). This has been demonstrated for both the transport of individual grain size fractions within mixtures (Figure 2a), as well as for the total combined transport of all sizes within said mixtures (Figures 2b and 3). Comparisons also demonstrate that the model maintains reasonable accuracy at the limit of uniform sediment grains (Figure 2c), covering a similar range in sediment sizes as comprising the considered mixtures.

3.2. *Influence of selected parameters*

With the full model validated in the previous sub-section for predicting wave-induced transport of graded and uniform sediments beneath velocity-skewed free stream wave signals, we will now investigate the sensitivity in the predictive accuracy to changes in some selected parameters. For this purpose, we will repeat the comparisons made in Figure 2a and 2b, but now with either the exposure factor or the reference concentration modification switched off (corresponding to setting either h_c=0 or Γ=0, respectively).

The effect of switching off the so-called exposure factor, again achieved simply by setting h_c=0, is depicted in Figure 4. It can be noted that there are only two sub-plots in this figure, as the exposure factor only affects cases involving graded sediments; the uniform sediment results are therefore identical to Figure 2c, and are thus not repeated. Comparing the results shown in Figure 4 with those shown in Figure 2a and 2b, it is evident that switching off this feature has a detrimental effect in the predicted transport rates, particularly for the larger grains; this makes intuitive sense as this parameter is designed to account for their increased exposure. As this parameter is applied directly onto the effective Shields parameter, it therefore inflates both the bed load transport rates, in addition to the reference concentrations. For the finer grains, the exposure factor does not have strong influence, however, as the ratio d_i /d_{50} is much closer to unity for these fractions.

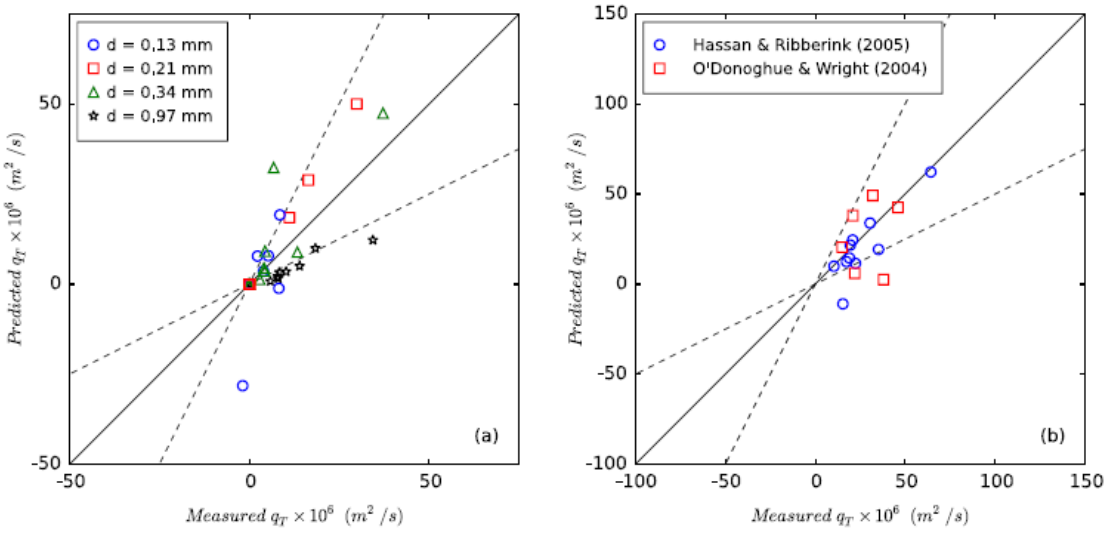

Figure 4. Summary of measured versus predicted (using h_c=0) period-averaged sediment transport rates, based on skewed-wave experiments of HR and OW. Sub-plot (a) compares transport rates for individual weight fractions (from HR), while (b) compares total transport rates of mixtures (both HR and OW). This figure is reprinted from Caliskan and Fuhrman (2017) with permission from Elsevier.

We finally investigate the effect of switching off the reference concentration modification (7), again achieved simply by setting Γ=0. As before, the uniform sediment results under this set up are identical to those in Figure 2c, and are not repeated. The resulting transport rates for the graded sediment mixtures are shown in Figure 5. As seen there, switching off this modification leads to a systematic under-prediction of the transport rates for the larger grain fractions (d=0.34 mm and d=0.97 mm in Figure 5a). The resulting total net transport rates for the graded sediments, presented in Figure 5b, are considerably worse than when this modification is included, Figure 2b; indeed, switching this feature off results in several predictions having the incorrect direction (sign) of the net transport. The net effect of this modification is to increase (decrease) the coarser (finer) fractions put into suspension. Based on the present results, this modification in particular helps to remedy an otherwise systematic tendency towards over-(under-) predicting the transport rates of fine (coarse) grain fractions, bringing both to approximately within a factor of two of measurements.

Note that Caliskan and Fuhrman (2017) additionally consider the effects of switching from the default settings to either μ_d=1 or β_s=1. The effects of changing the coefficient of dynamic friction, μ_d, was round to be fairly insignificant, whereas reducing β_s was found to result in under-predicted suspended transports for both uniform grained sediments as well as mixtures. Caliskan and Fuhrman (2017) also considered simulations involving gradation effects beneath so-called acceleration-skewed free stream flows. For full details on these additional investigations, please see their full paper.

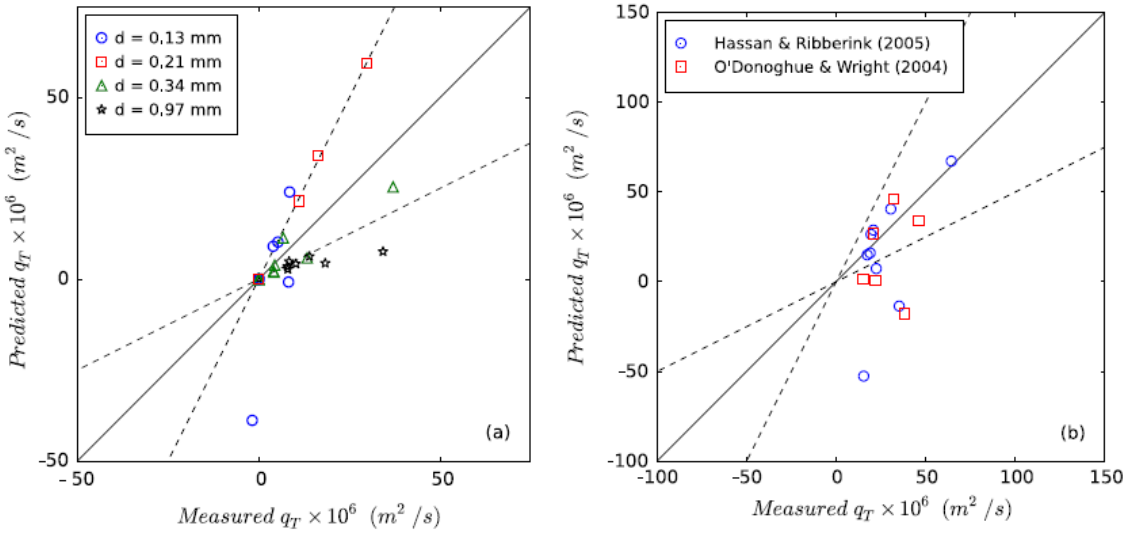

Figure 5. Summary of measured versus predicted (using Γ=0) period-averaged sediment transport rates, based on skewed-wave experiments of HR and OW. Sub-plot (a) compares transport rates for individual weight fractions (from HR), while (b) compares total transport rates of mixtures (both HR and OW). This figure is reprinted from Caliskan and Fuhrman (2017) with permission from Elsevier.

4. Conclusions

This paper presents a one-dimensional vertical (1DV) numerical boundary layer and sediment transport model. The model is based on the horizontal component of the Reynolds-averaged Navier–Stokes (RANS) equations, coupled with two-equation k–ω turbulence closure, which in turn drive bed and suspended sediment transport. The developed model extends the uniform sediment grain size model of Fuhrman et al. (2013) to incorporate multiple grain fractions e.g. for simulations involving well-graded sediment mixtures. The sediment transport model is based on individual bed and suspended load (based on turbulent-diffusion equation) descriptions for each grain fraction, and likewise includes so-called "high concentration effects" of turbulence suppression as well as hindered settling velocities. The model also accounts for: (1) increased flow exposure of coarse grain fractions on well-graded sediment beds, as well as (2) modification of the reference concentrations for applications at a fixed reference level (herein universally placed at b=2d_{50}). Parametric testing has revealed the importance of these factors, which combined to help alleviate the systematic over- and under-prediction of transported fine and coarse sand fractions, respectively. Of the two, the modified reference concentration has been found to be more significant.

As validation of the model net sediment transport rate predictions have been compared with those from oscillating tunnel measurements of O'Donoghue and Wright (2004, denoted OW herein) and Hassan and Ribberink (2005, denoted HR herein), who considered the transport of both well-sorted and graded sediments beneath velocity skewed wave signals. The model demonstrates acceptable accuracy (period-averaged predictions generally within a factor of two) for the predicted transport of both uniform, as well as graded, sediments. This is based on comparison with both total net transport measurements (HR and OW), as well as the net transports of individual grain fractions (as reported by HR). Comparison with the graded sediment experiments of HR has confirmed an effectively linear growth of the total net sediment transport versus the third moment of the free stream velocity for mixtures free of fine sand. The model likewise predicts deviations from this linear trend for mixtures involving fine sand, consistent with experimental observations. The reason for this deviation has been confirmed as being due to unsteady phase lag effects, which can reverse the dominant transport direction (to negative) of the fine sand fraction.

The model presented herein is an extension of the "MatRANS" model originally developed by Fuhrman et al. (2013). The code (developed in Matlab, with numerous examples) is freely available, upon request to the first author. This paper is an abridged version of the full journal paper of Caliskan and Fuhrman (2017), and for further results and discussion the interested reader is directed there.

References

Amoudry, L., Hsu, T.-J. and Liu, P.L.-F., 2008. Two-phase model for sand transport in sheet flow regime, J. Geophys. Res. 113, article no. C03011.

Caliskan, U. and Fuhrman, D.R., 2017. RANS-based simulation of wave-induced sheet-flow transport of graded sediments. *Coast. Eng*. 121, 90—102.

Davies, A.G. and Li, Z., 1997. Modelling sediment transport beneath regular symmetrical and asymmetrical waves above a plane bed. *Cont. Shelf Res.* 17, 555–582.

Engelund, F. and Fredsøe, J., 1976. A sediment transport model for straight alluvial channels. *Nordic Hydrol.* 7, 293—306.

Fredsøe, J. and Deigaard, R., 1992. *Mechanics of Coastal Sediment Transport.* World Scientific.

Fuhrman, D.R., Schløer, S. and Sterner, J., 2013. RANS-based simulation of turbulent wave boundary layer and sheet-flow sediment transport processes. *Coast. Eng.* 73, 151—166.

Hassan, W.N. and Ribberink, J.S., 2005. Transport processes of uniform and mixed sands in oscillatory sheet flow. *Coast. Eng.* 52, 745—770.

Holmedal, L.E. and Myrhaug, D., 2006. Boundary layer flow and net sediment transport beneath asymmetrical waves, *Cont. Shelf Res*. 26, 252–268.

Kranenburg, W.M., Ribberink, J.S., Schretlen, J.L.L.M. and Uittenbogaard, R.E., 2013. Sand transport beneath waves: the role of progressive wave streaming and other free surface effects. *J. Geophys. Res.* 118, 122–139.

Li, Z. and Davies, A.G., 2001. Turbulence closure modelling of sediment transport beneath large waves. *Cont. Shelf Res.* 21, 243—262.

Nielsen, P. and Callaghan, D.P., 2003. Shear stress and sediment transport calculations for sheet flow under waves, *Coast. Eng.* 47, 347–354.

O'Donoghue, T. and Wright, S., 2004. Flow tunnel measurements of velocities and sand flux in oscillatory sheet flow for well-sorted and graded sands. *Coast Eng.* 51, 1163—1184.

Silva, P.A., Abreau, T., van der A, D.A., Sancho, F., Ruessink, B.G., van der Werf, J. and Ribberink, J.S., 2011. Sediment transport in nonlinear skewed oscillatory flows: Transkew experiments, *J. Hydraul. Res.* 49, 72–80.

van der A, D.A., Ribberink, J.S., van der Werf, J.J., O'Donoghue, T., Buijsrogge, R.H., and Kranenburg, W.M., 2013. Practical sand transport formula for non-breaking waves and current. *Coast. Eng.* 76, 26–42.

van der Werf, J.J., Schretlen, J.J.L.M., Ribberink, J.S., O'Donoghue, T., 2009. Database of full-scale laboratory experiments on wave-driven sand transport processes. *Coast. Eng.* 56, 726–732.

van Rijn, L.C., 2007. Unified view of sediment transport by currents and waves III: graded beds, *J. Hydraul. Eng.* 133, 761–775.

Wilcox, D.C., 2006. *Turbulence Modelling for CFD*. DCI Industries.

Wu, W. and Lin, W., 2014. Nonuniform sediment transport under non-breaking waves and current. *Coast. Eng.* 90, 1–11.

Zyserman, J.A. and Fredsøe, J., 1994a. Data analysis of bed concentration of suspended sediment, J. Hydraul. Eng 120, 1021–1042.

Zyserman, J.A. and Fredsøe, J. 1994b. Bed concentration of suspended sediment and total load transport in asymmetric oscillatory flow. In: Book of Abstracts, Overall Workshop MAST, Gregynog, Wales.